Simple model for strong-laser-field ionization

Jakub Zakrzewski*
Department of Chemistry, University of Southern California, Los Angeles, California 90089-0482

Karol Życzkowski
Institute of Physics, Jagiellonian University, ul. Reymonta 4, 30-059 Krakow, Poland
(Received 31 March 1987)

A simple model of ionization, capable of dealing with arbitrarily strong laser fields, is discussed. A model "atom," consisting of a rectangular well potential of finite depth is perturbed by a train of δ kicks that are alternating in sign. The results of exact (numerical) calculations are compared with those obtained neglecting continuum-continuum transitions. Both the ionization rate and the photoelectron spectra are discussed. Neglecting continuum-continuum transitions leads to good results for the ionization rate which is well approximated by the low-field perturbative expression up to very strong fields. On the contrary photoelectron spectra are sensitive to a detailed form of continuum-continuum matrix elements (both to their singular and regular parts).

I. INTRODUCTION

Strong-laser-field ionization belongs to the most intensively studied problems in multiphoton physics. Although the first attempts to tackle the problem were made in the 1960s,[1,2] the phenomenon is far from being understood completely. Continuing theoretical efforts in the last twenty years[3] have been mainly devoted to calculation of the ionization rate, mostly for "nonresonant" ionization (i.e., with no intermediate bound-bound resonance).

Recently, however, it has become possible to measure in detail the energy distribution of the ejected electrons.[4] It turned out that the electron energy spectra consisted of several equally spaced peaks centered at energies corresponding to the absorption of photons beyond the minimum number N required for ionization. With increasing intensity the lowest (in energy) peaks disappear and the center of the remaining peaks' envelope moves to higher energies. The phenomenon, termed above-threshold ionization (ATI) stimulated intensive theoretical studies in the last few years. Several different models have been proposed in order to explain the disappearance of the lowest peaks. In the first approach[5] the large ac shifts induced by a strong laser field increase the electron binding energy thus making the lowest $N, N+1, \ldots$ processes forbidden energetically. The ponderomotive force[6] which affects the electron motion while it is leaving the laser pulse compensates the ac shifts; in this way the model[5] explains the position of the peaks at their field-free values. This model has been further advanced by several authors.[7] The other approach, which does not take into account the effects of the ponderomotive force, was proposed by Reiss[8(a)] and later independently by Bialynicka-Birula[8(b)] and also received a lot of attention.[9] This approach is sometimes called the essential states approach (ESA).[9(e)]. In this approach one defines the effective bound-continuum and continuum-continuum matrix elements and then attempts to solve the resulting problem nonperturbatively. The different variations of the method[8,9] differ primarily in the assumed form of these matrix elements. The *total* disappearance of many of the lowest electron peaks in this approach has yet to be shown, but the model predicts the overall shift of the peaks' envelope and qualitatively agrees with the experiments. It was pointed out also[10] that space-charge effects may be responsible for the disappearance of the lowest-energy peaks; however, in most recent experiments[11] the disappearance of the peaks persists despite efforts to minimize the space-charge effects.

Clearly, more studies are needed to clarify the relative role played by different possible mechanisms. The most direct method, straight integration of the Schrödinger equation resulting from the exact Hamiltonian for the realistic atom, is still quite costly and does not give, at present, reliable results.[12] Therefore, there seems to be an urgent need for studies of simplified models which, however, can be exactly solved without assuming the form of matrix elements. These may serve then as a tests of several versions of ESA. In the seventies Geltman[13] discussed the laser-field ionization of a model one-dimensional atom. The atomic potential was modeled by a δ function. Geltman concentrated on the ionization rate studies only. Austin[14] obtained for the first time (as far as we know) the multiplicity of electron energy peaks within the same model by straightforward integration of the Schrödinger equation. Quite recently, Blumel and Meir[15] were able to follow exactly the system evolution (for the δ potential) by approximating the harmonic perturbation by a train of δ kicks alternating in sign. They compared the full solution with the results obtained by neglecting the continuum-continuum transitions and found the latter approximation to be an excellent one as far as the ionization rate is concerned.

The findings of Blumel and Meir,[15] contradictory in some sense to the ESA basic results, came as a surprise. However, as the atomic potential studied by them is ex-

tremely short ranged, it is dangerous to draw any definite conclusions about real-atom ionization from their results. In the δ model the electron in the continuum is almost free and as such cannot emit or absorb photons.

To shine some light on this discrepancy we have studied a similar one-dimensional model potential, namely the square-well potential (preliminary results have been presented elsewhere[16]). This potential is also short ranged—thus more suitable for studies of negative ions rather than neutral atoms. However, by changing the well width we are able to study the influence of the potential range on the applicability of the approximation which neglects continuum-continuum transitions (NCCTA). The square-well potential was used by Austin[14] in the context of one-photon resonant two-photon ionization.

The ionization from the square-well one-dimensional potential is also of interest for its own rights. Such a potential may well describe electrons trapped in the potential well of semiconducting layered structures (see Ref. 17 and references therein)—the so-called quantum wells—that are currently under intensive studies in semiconductor physics.[18] It has also been pointed out[17] that ionization from a square well may serve as a simple (if not the simplest) system to study quantum stochasticity.

The model studied is defined in Sec. II, where we address also the numerical details. The results are presented and discussed in Sec. III. We conclude the results and discuss future perspectives in Sec. IV. In the Appendixes we give the necessary formulas for the square-well potential and present the expressions for the matrix elements.

II. THE MODEL

The one-dimensional model discussed is defined by the Hamiltonian

$$H=H_0+V(x)\ , \tag{1}$$

where H_0 describes the "atomic" part of H:

$$H_0=p^2/2m+V(x) \tag{1a}$$

and $V(x)=-V$ for $|x|<A$, $V(x)=0$ otherwise. V and A are the well depth and width, respectively. The interaction with the electromagnetic field is approximated by

$$H_1=eEx\sum_k(-1)^k\delta(t-kT/2)\ , \tag{1b}$$

where E is the amplitude of the field and the sinusoidal perturbation with frequency $\omega_L=2\pi/T$ is approximated by a train of δ kicks alternating in sign. Such an approximation is well known from studies of microwave ionization of the hydrogen atom[19] and was applied by Blumel and Meir[15] in their treatment of δ-potential ionization. The Hamiltonian (1) is periodic with period T, however, as

$$\sum_k(-1)^k\delta(t-kT/2)=\frac{2}{T}\sum_{n=-\infty}^{+\infty}\exp[2\pi i(2n+1)t/T]\ , \tag{2}$$

the perturbation contains all odd harmonics of the basic frequency ω_L.

The beauty of the δ-kick approximation of the sinusoidal perturbation lies in the fact that we know exactly the evolution of the system between kicks (governed by the field-free part of the Hamiltonian H_0). On the other hand at $t=kT/2$ (during the kick) the influence of H_0 is negligible. Thus from the Schrödinger equation we can easily obtain the corresponding quantum map[20] in a way similar to that applied for the celebrated kicked quantum rotor:[21]

$$\psi_{n+1}=\exp(-igx)\exp\left[-\frac{iT}{2\hbar}H_0\right]\exp(igx)\times\exp\left[-\frac{iT}{2\hbar}H_0\right]\psi_n\ , \tag{3}$$

where $g=eET/2\hbar$ and ψ_0 corresponds to the initial atomic state at $t=0$ which we choose to be the ground state.

To evaluate the map (3) we work within the basis of eigenfunctions of H_0. The square-well potential is a standard example in many textbooks devoted to quantum mechanics; nevertheless, we have accumulated in Appendix A all the necessary formulas [i.e., bound and continuum functions of $V(x)$] in order to establish the unified notation and for completeness. In this basis the evolution operator between impulses is diagonal. Thus we only have to determine the kick-evolution operator $U_{\text{kick}}=\exp(\pm igx)$ matrix elements. These are straightforward to calculate, but the results are unfortunately rather lengthy (see Appendix B for an example). However, some properties of the matrix elements may be obtained by simple considerations only. Expanding operator $\exp(igx)$ in the power series $\exp(igx)=1+igx-g^2x^2/2+\ldots$, we notice that the zero-order (in g) contribution reproduces the free evolution (in the infinitely short time of the pulse). The first-order term igx couples the states of opposite parity only. The first-order matrix elements are identical to those corresponding to continuous harmonic perturbation (but in our case acting at discrete times $t=kT/2$, $k=1,2,\ldots$). In the second order, states of the same parity become coupled directly, that, however, being the case for relatively large g and mainly for delocalized, continuum states (when large values of x become important). Thus we may expect that second- and higher-order (in g) terms will play a significant role in exact results and less so in NCCTA where no continuum-continuum interaction is allowed for. In Appendix B we present an exemplary exact matrix element between continuum states. Note that it consists of regular and singular parts. The singular parts are centered at $(g\pm s\pm s')$. This will turn out to be of great importance for the shape of photoelectron spectra obtained. Let us stress here only that the corresponding singular parts for the igx operator (continuous

perturbation) are located at $(s \pm s')$, i.e., their positions are g independent.

To save space we do not present formulas for bound-continuum matrix elements either. Their behavior as a function of continuum state energy ω is important, however, for understanding the spectra so we describe them qualitatively. The modulus square of the matrix element first linearly increases with ω from its zero value at threshold (as opposed to $\omega^{l+1/2}$ Wigner law for short-range three-dimensional potentials). For larger ω it saturates and later decreases to zero value for large ω. Typically for the same initial bound energy this decrease is more rapid for a wide square well and less rapid for the narrow well.

To follow the evolution of the system on a computer we had to discretize the continuous part of the "atomic" energy spectrum. Several methods of discretization have been tried. We have found the oldest method—putting the system in a large box of size $2L$—to be most reliable (the same method was applied by Austin[14] and Blumel and Meir[15]). It is well known that finite spacings of levels in the "quasicontinuum" may lead to quantum recurrences (related in our case to reflections on the walls of the box). Those were avoided by choosing L large enough to assure convergence of the results. Finally we had to introduce a high-energy artificial cutoff, carefully chosen to assure that the states with higher energy may be safely ignored. The choice of the cutoff value was controlled by the preservation of the wave-function normalization during the time evolution. For about 30 field periods, $L = 500A$ (corresponding to about 1200 states in the quasicontinuum) was sufficient to obtain good convergence in the most demanding small frequency cases.

The calculations were performed on a CDC 6400 computer. Calculation of the matrix elements of the kick-evolution operator was the most time consuming operation. These matrix elements were stored on disk and used consecutively in rows (as the available memory was too small to hold the whole matrix).

III. RESULTS

The results presented correspond to the model with one bound state only. The numerical treatment of the potential supporting more bound states does not involve any additional difficulties (the continuum part is the most demanding); however, we have constrained ourselves to the one-level model for clarity. Such a model allows for direct comparison of results with that obtained with the δ-potential model.[15] Moreover, such additional effects as Rabi oscillations between bound states, competition between resonant and nonresonant processes, etc., are avoided, thus providing a simple clear picture of the ionization process.

Following Blumel and Meir[15] we parametrize the perturbation strength via dimensionless parameter $\beta = g/\gamma = eET/2\hbar\gamma$, where γ is the decay coefficient of the bound state wave function outside the well [see (A1)]. The laser frequency ω_L is measured in the units of bound energy $|E_0|$; thus $\omega_L = 1$ corresponds to the one-photon ionization threshold.

A. Ionization rate

The dependence of the ionization rate on β is presented in Fig. 1. Figure 1(a) corresponds to $\omega_L = 1.25$ (one-photon ionization), while Fig. 1(b) to $\omega_L = 0.7$. The ionization rate has been calculated by a fit to the expression $|\langle \psi_{b,n} | \psi_{b,n} \rangle|^2 = \exp(-Rt_n)$, where $t_n = nT$, $n = 0, 1, \ldots$ is a discretized time and $\psi_{b,n}$ is a projection of the ψ_n onto the bound, initial state. The fit of such obtained rates to the low-intensity power law $R = \text{const}\beta^{2\alpha}$ is presented as a straight line in Fig. 1. For $\omega_L = 1.25$ the fitted value of $\alpha = 1.003$ supports the one-photon ionization picture. We have compared the exact results with that obtained using NCCTA. Up to $\beta = 0.2$ NCCTA agrees well with the exact results. A

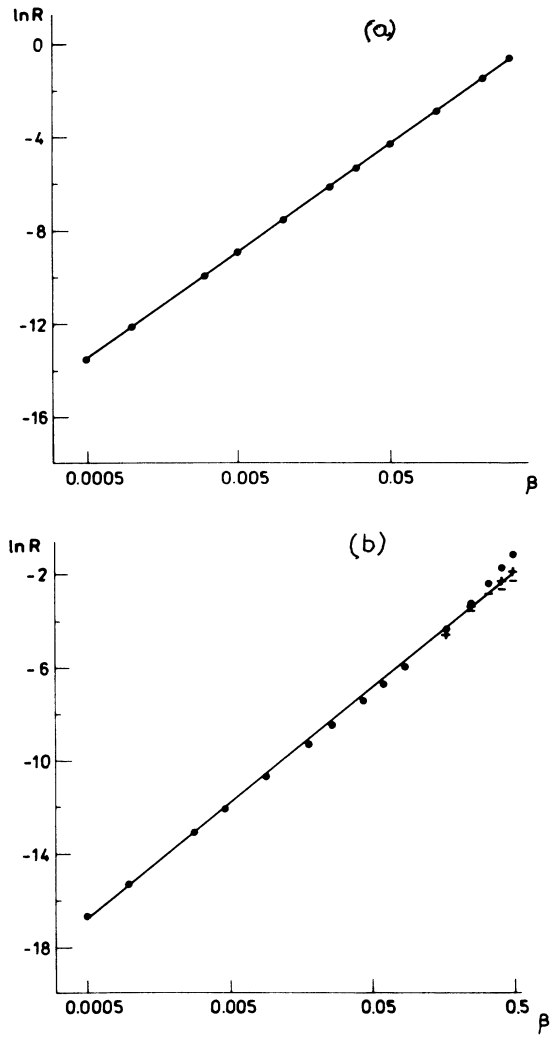

FIG. 1. The ionization rate as a function of dimensionless perturbation strength β (log-log plot). Solid circles, rates obtained from exact calculations (as described in text); solid line, fit of power law $R = \text{const} \cdot \beta^{2\alpha}$. The perturbation frequency equals $\omega_L = 1.25\,|E_0|$ in (a) and $\omega_L = 0.7\,|E_0|$ in (b). Pluses correspond to "bound" NCCTA, minuses to "continuum" NCCTA (b).

similar fit for $\omega_L=0.7$ [Fig. 1(b)] gave $\alpha=1.07$ indicating also a one-photon process. This should not be surprising as the Fourier expansion [Eq. (2)] shows the presence of all odd $3\omega_L, 5\omega_L, \ldots$ harmonics in the perturbation. Thus the value of α obtained tells us that in this case ionization is dominated by a one-photon process with frequency $3\omega_L$.

We have denoted by + and − the results obtained within NCCTA (whenever different from exact results) in Fig. 1(b). Two values obtained for each (large) β correspond to two possible ways of calculating the rate. The +'s correspond to the method based on the decay of the bound state (described above, later referred to as "bound" NCCTA); −'s are obtained by calculating the increase of the norm of the "continuum part" of the wave function ("continuum" NCCTA). Whenever the normalization of the wave vector is conserved (it is always in the exact calculations), both methods are equivalent. However, the breakdown of the NCCTA manifests itself in the deviation of the corresponding norm from unity. Thus we have found it useful to calculate the rate in these cases by both methods.

From a few studies of intensity dependence of the ionization rate (see also Ref. 16) it is clear that the NCCTA holds very well as far as the ionization rate is concerned. For very strong perturbation the rate obtained by the "bound state" method within NCCTA gives better results than the "continuum" method [compare Fig. 1(b)]. In this range of β, ionization rates obtained applying NCCTA underestimate exact results. Let us point out that we *did not* observe any saturation of the ionization rate, which is typical of Keldysh[1]-like strong field treatments. For a strictly one-photon process [compare Fig. 1(a)] the low-field perturbative rate holds perfectly well up to very strong fields.

Ionization rate dependence on the laser frequency ω_L is presented in Figs. 2 and 3 for "narrow" (Fig. 2) and "wide" (Fig. 3) potential well. The thresholds for one-photon ionization at $\omega_L=1$ and $\omega_L=\frac{1}{3}$, the latter corresponding to ionization by a third harmonic of the perturbation [see (2)], are quite pronounced. The dots correspond to exact results, solid lines give NCCTA estimates that are quite accurate for the $\beta=0.1$ value in the whole range of frequencies shown.[22] The well parameters were chosen to assure that the bound level energy was $E_0=-0.5$ a.u.; thus $\beta=0.1$ corresponded in both cases to the same values of kicking strength g. Note that ionization is more effective for "wide" (Fig. 3) well [except for a small region just below the threshold, where ionization rates are less accurate (see below)]; also the threshold behavior is sharper in this case. The dotted line in Fig. 3 indicates the rate obtained by continuum NCCTA; thus in the region of most effective ionization (maximal bound-free matrix element) the NCCTA breaks down partially even for $\beta=0.1$. The vertical slashed lines indicate the region of frequencies just below the threshold, where the decay of ground-state population is *strongly* nonexponential (both for exact and NCCTA calculations). Thus the rates calculated in this frequency interval are much less accurate. This nonexponential decay seems to be typical for near-threshold ionization in the short-range potential (similar behavior was predicted for negative ions from Wigner-type threshold law behavior[23]). We will study this effect in detail elsewhere, as it is interesting for the semiconductor physics application of this model.

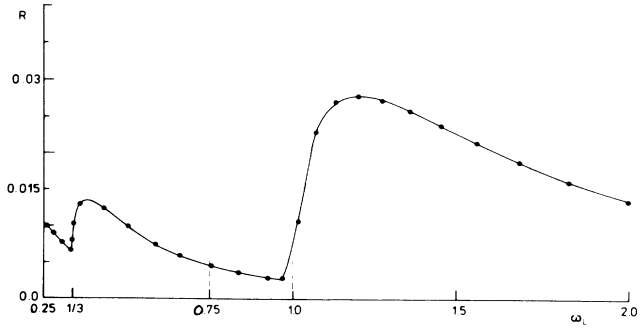

FIG. 2. Ionization rate as a function of the field frequency for $\beta=0.1$ for "narrow" square well: $A=0.1$ a.u., $V=5.33$ a.u., $|E_0|=0.5$. Solid circles represent exact results; solid curve, "bound" NCCTA. For further explanation see text.

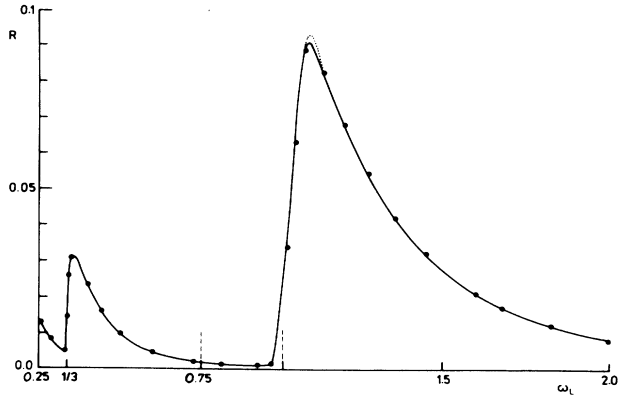

FIG. 3. Same as Fig. 2 for "wide" well: $A=1$, $V=0.87$, $|E_0|=0.5$. The dashed line close to maximum shows results of "continuum" NCCTA where they are different from "bound" NCCTA results.

Summarizing our ionization rate results, we may say that, as far as the ionization rate is concerned, the NCCTA approximation works very well for moderately strong β. This supports previously reached conclusions.[15]

B. The photoelectron spectra and the wave function behavior

As mentioned before, the continuum of scattering states has been discretized by putting the system in the large box of size $2L$. This procedure lifts the degeneracy of even and odd continuum states (see Appendix A). In order to obtain the realistic spectrum, the following final states procedure has been applied: Evolution of the system in the box determines amplitudes $\beta^o(\omega_n^o,t)$,$\beta^e(\omega_n^e,t)$ where superscripts e,o denote even and odd "quasicon-

tinuum" states, and n denotes the nth pair of states. These two amplitudes allow us to obtain the probability for an electron having energy $\omega_n=(\omega_n^e+\omega_n^o)/2$ via

$$W(\omega)=|\beta^o(\omega_n^o,t)|^2+|\beta^e(\omega_n^e,t)|^2 ,$$

i.e., two states of opposite parity provide one point of the spectrum $W(\omega)$ at the averaged energy.

The exemplary spectra obtained are shown in Figs. 4 and 5 and Figs. 6 and 7 for "narrow" and "wide" well, respectively.[24] The spectra obtained from exact calculations (Figs. 4 and 6) are to be compared with that (Figs. 5 and 7) calculated with NCCTA. All presented spectra were calculated for $\beta=0.1$, i.e., for the case in which NCCTA has worked very well as far as the ionization rate had been concerned. The frequency ω_L was chosen just below the one-photon ionization threshold to minimize to some extent the ionization rate (which should make NCCTA work even better). The NCCTA spectra (Figs. 5 and 7) show pronounced peaks corresponding to excitation by different harmonics of the perturbation (thus, as ω_L is defined in the units of $|E_0|$, the $3\omega_L$ peak is centered at $\omega=0.95$ a.u., the $5\omega_L$ peak at $\omega=1.92$, etc.). The envelope of the peaks corresponds roughly to the square of the absolute value of the bound-free matrix element between the even bound state and odd quasicontinuum states (in NCCTA 98% of continuum excitation is within the odd parity subspace[25]). The residual excitation close to $\omega=0$ comes from one-photon excitation by the ω_L harmonic. The spectra obtained in exact calculations (Figs. 4 and 6) show two features which are drastically different from NCCTA curves (Figs. 5 and 6). Firstly, apart from $(2n+1)\omega_L$ peaks we observe now peaks at $2n\omega_L$ originating from the continuum-continuum interaction. Secondly, each peak in the exact spectrum is split into a doublet, with splitting increasing with ω. It is straightforward to associate this splitting with the singular part of the continuum-continuum matrix element of the kick operator (see Appendix B). The state with energy ω is coupled, by the singular part, to, e.g., state ω', such that (see Appendix A) $s'=s+g$. For large ω,ω' the singular part

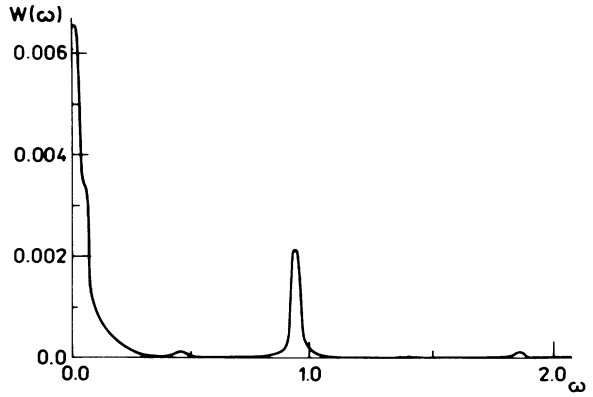

FIG. 5. Spectra obtained within NCCTA for the same values of parameters as in Fig. 4.

couples ω and $\omega'=\omega+2g(\omega)^{1/2}$. Comparing spectra obtained for different g (i.e., β), we have confirmed the linear dependence of the splittings on β at given energy ω. It should be stressed once more that this splitting is a peculiarity of δ perturbation and may not be observed with realistic sinusoidal perturbation. It is to be noted that although the "exact" and NCCTA spectra are very different the peaks corresponding to one-photon excitation by $(2n+1)$ harmonics are still dominant in the exact spectra. We have varied both the frequency of perturbation ω_L and its strength β but we were unable to induce "peak switching," so prominent in ATI experiments. We shall comment on this in the concluding section.

One more interesting feature of the calculated spectra should be noticed. Note that both NCCTA spectra show small bumps at ω corresponding to excitation with frequency $2\omega_L$. This frequency is not present in the perturbation so these small peaks come as a surprise. We have verified that their presence is not due to finite times at which spectra are calculated (the finite train of δ-kicks may have some residual even-parity ω_L Fourier components); the bumps do not disappear for longer interac-

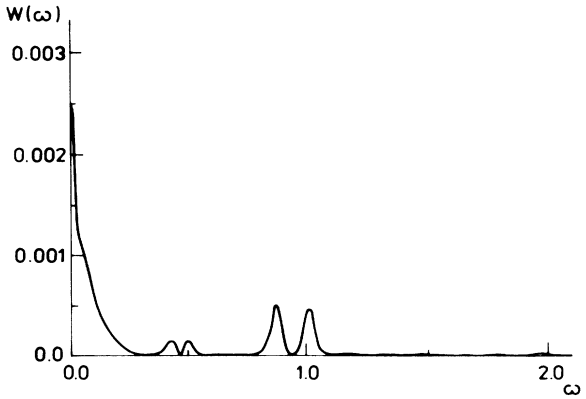

FIG. 4. Exact photoelectron spectra obtained for "wide" well: $\beta=0.1$, $\omega_L=0.97|E_0|$. Note the pronounced splitting due to singular part of the kick-evolution operator.

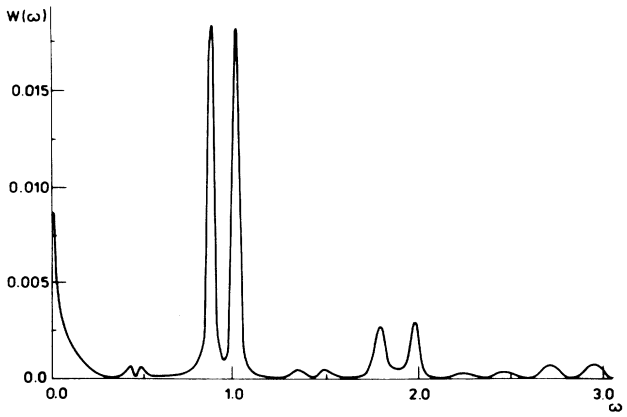

FIG. 6. Exact photoelectron spectra for "narrow" well: ω_L, β as in Fig. 4.

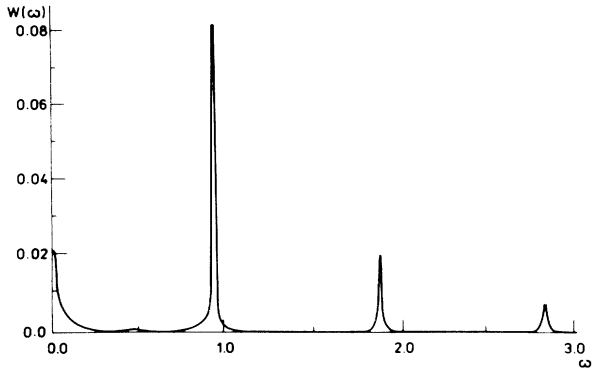

FIG. 7. Spectra obtained with NCCTA for the same values of parameters as in Fig. 6.

tion times. The only plausible explanation of their existence seems to be the effect of direct tunneling from ground state—the effect predicted by Keldysh.[1]

The calculation method allowed us to follow the evolution of the wave function. We present the time evolution of the probability density in Fig. 8. The electrons leave the well in "packets" almost symmetrically in both directions. We have allowed for a rather strong perturbation strength here to have a sufficient depletion of the initial state. The smooth symmetric curve presented was obtained within NCCTA. Exact calculations show additional small wiggles superimposed on an envelope similar to that presented in Fig. 8. The real difference between NCCTA and exact wave functions may be seen when real or imaginary parts of the corresponding wave functions are compared. As an example, we show the real part of the continuum component of the wave function (we plot $|\langle\psi(t)|Q\psi(t)\rangle|^2$ where Q is the projection operator into quasicontinuum, i.e., $Q=1-P$, $P=|\psi_B\rangle\langle\psi_B|$) in Fig. 9. Note that the curve corresponding to NCCTA is almost antisymmetric. As mentioned above, within this approximation, the odd quasicontinuum states are mostly excited.[25] The slight distortions are due to the higher order in g terms (see discussion of the kicking operator in Sec. II). The exact wave functions show much richer structure with no apparent symmetries. It is due to almost equal (as confirmed by numerical integration) excitation of odd and even quasicontinuum states—showing the importance of continuum-continuum transitions.

IV. CONCLUSIONS

We have studied the exactly soluble model of the electron bound in the finite rectangular well potential and perturbed by a train of δ kicks that are alternating in sign. We have compared the exact results with that obtained by neglecting continuum-continuum transitions (NCCTA). We have confirmed the results of Blumel and Meir[15] (obtained for an extremely short-ranged atomic potential)—namely, that NCCTA works quite well as far as the ionization rate is concerned. On the other hand, we have shown that the photoelectron spectra obtained within both models (the exact one and NCCTA) differ drastically. Thus it may be said that (at least in our model) bound-continuum and continuum-continuum transitions are in some sense "separated." Both the singular and the regular part of the continuum-continuum interaction seem important in obtaining the spectra. Up till now the ESA models[9] of ATI have either included the former or the latter part of the matrix elements. We have tried to separate the effects induced by these parts by, say, neglecting the singular part (leaving the regular part only) or vice versa. It has turned out, however, that for reasonable field strengths β, for which at least partial ionization occurred (β larger than 0.01), the normalization of the wave vector was not preserved in such simplified models. It suggests that

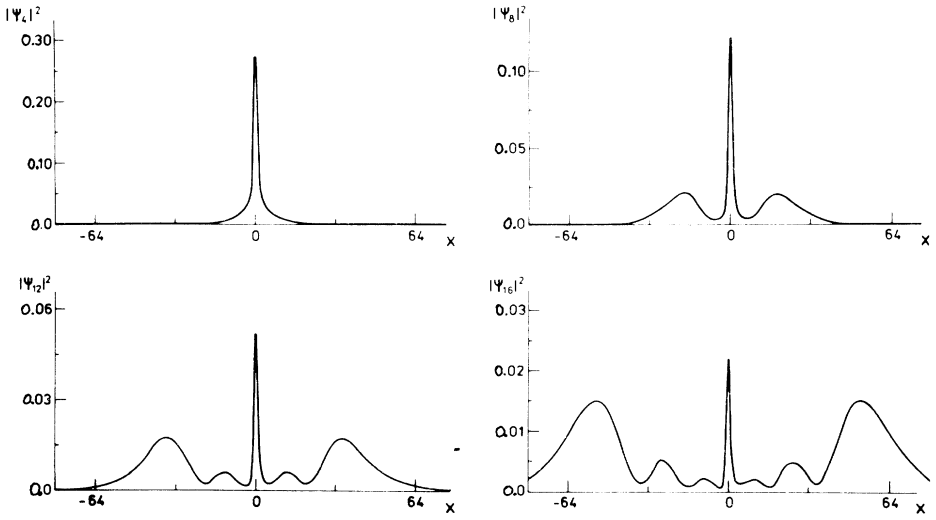

FIG. 8. Evolution of the probability density $|\langle\psi(x,t)|\psi(x,t)\rangle|^2$ after $n=4,8,12,16$ field periods; $\beta=0.2$, $\omega_L=1.25|E_0|$, "wide" well case. The box size $L=200$ is sufficient to avoid reflections on box walls (NCCTA result).

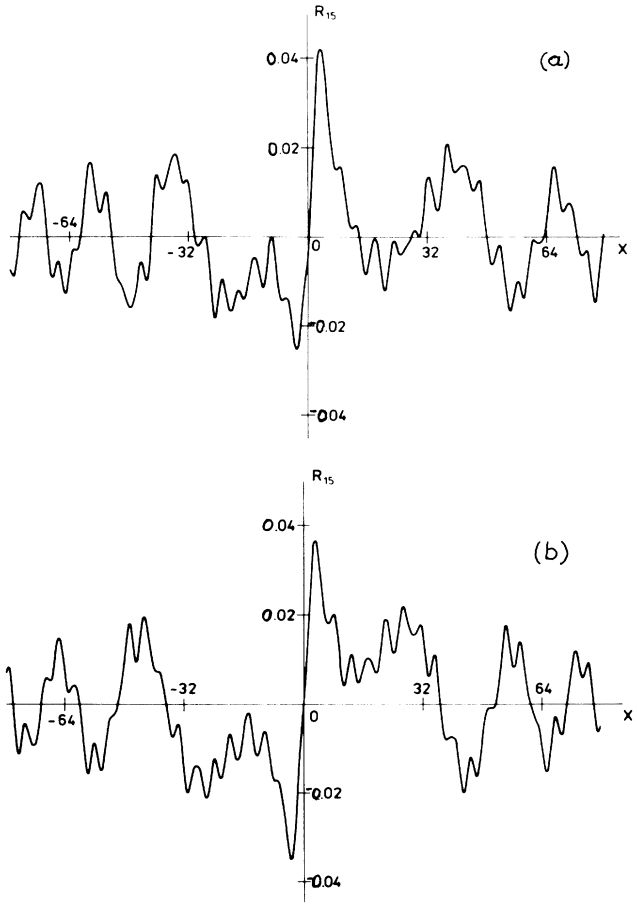

FIG. 9. The real part of the "continuum" projection of the wave function after 15 periods of the external field. (a), exact result; (b), NCCTA result. The values of parameters are $\beta=0.1$, $\omega_L=0.96\,|E_0|$, $A=1$, $V=0.87$ ("wide" well).

both regular and singular parts are of comparable importance and interfere with each other. Thus any study of ionization (more realistic than our simple model) requires careful modeling of the continuum-continuum matrix elements to take into account both of these parts.

The presence of a small peak around ω corresponding to $2\omega_L$ excitation in NCCTA spectra is an indication of the tunneling in the alternating field as suggested by Keldysh in his early study.[1]

Although the continuum-continuum interaction affects very strongly the photoelectron spectra, we have not observed signs of the "peak-switching" phenomenon so characteristic of ATI experiments. It well may be that it is due to the short-range character of potential studied. However, we have changed the potential range and we have not seen any significant changes in the spectra. On the other hand, the "peak-switching" observed in several experiments[4] is most prominent for multiphoton ionization (i.e., relatively low frequency photons). In our model the δ perturbation brings in photons of arbitrary large frequency. By decreasing ω_L we cannot induce significant changes as the higher harmonics present in the perturbation will always make one-photon ionization dominant. By applying the modulated kicks approximation, introduced recently,[26] one may be able to study multiphoton ionization even with δ-type perturbation. We are not able to perform such studies due to computer CPU and memory limitations.

Thus the alternating δ-kick approximation, although, we hope, useful in providing insight into the relative importance of various parts of continuum-continuum matrix elements (due to the peculiar, strength-dependent singular part), does not seem to be applicable in any more realistic study of strong field ionization.

ACKNOWLEDGMENTS

We are grateful to K. Rzazewski, J. Mostowski, and M. Lewenstein for several fruitful discussions. We thank H. S. Taylor for discussions and careful reading of the manuscript. This work has been supported in part by Polish Government Contract No. CPBP0107. One of us (J.Z.) acknowledges support by National Science Foundation Grant No. CHE-8511496.

APPENDIX A

Square well

Let us assume the one-dimensional potential $V(x)=-V$ for $|x|<A$, $V(x)=0$ otherwise. The potential is symmetric with respect to origin so the eigenvectors (nondegenerate) are of odd or even parity. For energy $E<0$ let us denote ($m=\hbar=1$): $\gamma^2=-2E$, $k^2=2(E+V)$. Then the even-parity eigenvalues are determined by condition $\gamma=k\tan(kA)$ and the corresponding eigenvectors are

$$\psi^e_\gamma(x)=\begin{cases}\exp(-\gamma|x|) & \text{for } |x|>A\ , \\ \dfrac{\exp(-\gamma A)}{\cos(kA)}\cos(kx) & \text{for } |x|<A\ .\end{cases} \tag{A1}$$

The odd eigenvalues are given by solutions of $\gamma=-k\cot(kA)$ and the corresponding eigenvectors are

$$\psi^o_\gamma(x)=\begin{cases}\dfrac{|x|}{x}\exp(-\gamma|x|) & \text{for } |x|>A\ , \\ \dfrac{\exp(-\gamma A)}{\sin(kA)}\sin(kx) & \text{for } |x|<A\ .\end{cases} \tag{A2}$$

In (A1) and (A2) the normalization constant equals to

$$B(\gamma)=\exp(\gamma A)[\gamma^{-1}+A+\gamma k^{-2}+A(\gamma/k)^2]^{-1/2}\ . \tag{A3}$$

The positive energy states form a double-degenerate continuum. Let us denote this time:

$$s^2=2\omega,\quad l^2=2(\omega+V)\ , \tag{A4}$$

where ω denotes the energy of a state. Properly normalized even and odd eigenstates may be build up from scattering "incoming" states:

$$\psi^e_\omega(x)=2^{-1/2}[\psi^L_\omega(x)+\psi^R_\omega(x)]\ ,$$
$$\psi^o_\omega(x)=2^{-1/2}[\psi^L_\omega(x)-\psi^R_\omega(x)]\ , \tag{A5}$$

where $\psi^L_\omega,\psi^R_\omega$ are properly normalized "incoming" states "from the left" and "from the right," respectively, i.e.,

$$\psi^L_\omega(x)=(2\pi)^{-1/2}\begin{cases} e^{isx}+S_{21}(\omega)e^{-isx} & \text{for } x<-A\ , \\ K(\omega)e^{ilx}+L(\omega)e^{-ilx} & \\ & \text{for } -A<x<A\ , \\ S_{11}(\omega)e^{isx} & \text{for } x>A\ . \end{cases} \tag{A6a}$$

and

$$\psi^R_\omega(x)=(2\pi)^{-1/2}\begin{cases} S_{22}(\omega)e^{-isx} & \text{for } x<-A\ , \\ L(\omega)e^{ilx}+K(\omega)e^{-ilx} & \\ & \text{for } -A<x<A\ , \\ e^{-isx}+S_{12}(\omega)e^{isx} & \text{for } x>A\ . \end{cases} \tag{A6b}$$

In (A6) $S_{ij}(\omega)$ are the S-matrix elements

$$S_{11}(\omega)=S_{22}(\omega)=\frac{\exp(-2isA)}{\cos(2lA)-i\epsilon\sin(2lA)}\ , \tag{A7a}$$

$$S_{12}(\omega)=-S_{21}(\omega)=i\eta\sin(2lA)\frac{\exp(-2isA)}{\cos(2lA)-i\epsilon\sin(2lA)}\ . \tag{A7b}$$

with $\epsilon=(s/l+l/s)/2$, $\eta=(s/l-l/s)/2$, and

$$K(\omega)=S_{11}(\omega)(1+s/l)\exp[i(s-l)A]/2\ ,$$
$$L(\omega)=S_{11}(\omega)(1-s/l)\exp[i(s+l)A]/2\ . \tag{A8}$$

Square well in the box

In the box approximation the potential takes the form $V(x)=-V$ for $|x|<A$, $V(x)=0$ for $A<|x|<L$, $V(x)=\infty$ for $|x|>L$. Provided $L\gg A$ the bound states are not affected by the presence of the box (as the wave functions are localized). On the other hand, the box discretizes the continuum producing quasicontinuum and lifts the degeneracy of states. The even-parity quasicontinuum states

$$\psi^e_\omega(x)=B^e(\omega)\begin{cases} \dfrac{\cos(lA)}{\sin[s(L-A)]}\sin[s(x+L)] & \\ & \text{for } -L<x<-A\ , \\ \cos(lx) \quad \text{for } -A<x<A\ , & \\ \dfrac{\cos(lA)}{\sin[s(L-A)]}\sin[s(L-x)] & \\ & \text{for } A<x<L \end{cases} \tag{A9}$$

have the energy ω determined via solution to

$$s=l\tan(lA)\tan[s(L-A)] \tag{A10}$$

[with s and l defined by (A4)] and the normalization constant is equal to

$$B^e(\omega)=\left[A+\frac{\sin(2lA)}{2l}(1-l^2/s^2)+\frac{\cos^2(lA)}{\sin^2[s(L-A)]}(L-A)\right]^{-1/2}\ . \tag{A11}$$

The odd-parity wave functions are given by

$$\psi^e_\omega(x)=B^e(\omega)\begin{cases} -\dfrac{\sin(lA)}{\sin[s(L-A)]}\sin[s(x+L)] & \\ & \text{for } -L<x<-A\ , \\ \sin(lx) \quad \text{for } -A<x<A\ , & \\ \dfrac{\sin(lA)}{\sin[s(L-A)]}\sin[s(L-x)] & \\ & \text{for } A<x<L \end{cases} \tag{A12}$$

with the corresponding eigenvalue condition

$$s=-l\cot(lA)\tan[s(L-A)] \tag{A13}$$

and normalization constant

$$B^o(\omega)=\left[A-\frac{\sin(2lA)}{2l}(1-l^2/s^2)+\frac{\sin^2(lA)}{\sin^2[s(L-A)]}(L-A)\right]^{-1/2}\ . \tag{A14}$$

APPENDIX B

The matrix elements of operator $\exp(\pm igx)$ between different eigenstates are quite lengthy, although straightforward, to calculate. The integrals involved are of the type

$$I=\int_a^b\exp(\pm\alpha x)\cos(kx)dx\ .$$

We do not present all the matrix elements here. As an example, discussed in the text we quote an exemplary formula for the free-free transition matrix element for the "pure" ($L=\infty$) square-well potential between incoming scattering states. Let us denote by s,l the wave numbers associated via (A4) with energy ω and by s',l' those corresponding to ω'. Then, e.g.,

$$\langle \psi_\omega^L \mid e^{igx} \mid \psi_\omega^R \rangle = \tfrac{1}{2}\{\delta(g-s-s')[S_{11}^*(\omega)+S_{22}(\omega')]+\delta(g+s-s')S_{22}(\omega')S_{21}^*(\omega)$$
$$+\delta(g-s'+s)S_{11}^*(\omega)S_{12}(\omega')\}$$
$$+\frac{i}{2\pi}S_{11}^*(\omega)\left[P\frac{\exp[i(g-s-s')A]}{g-s-s'}+S_{12}(\omega')P\frac{\exp[i(g-s+s')A]}{g-s+s'}\right]$$
$$-\frac{i}{2\pi}S_{22}(\omega')\left[P\frac{\exp[i(g-s-s')A]}{g-s-s'}+S_{21}^*(\omega)P\frac{\exp[i(g+s-s')A]}{g+s-s'}\right]$$
$$+\frac{1}{\pi}\left[K^*(\omega)\left[L(\omega')\frac{\sin[(g-l+l')A]}{g-l+l'}+K(\omega')\frac{\sin[(g-l-l')A]}{g-l-l'}\right]\right.$$
$$\left.+L^*(\omega)\left[L(\omega')\frac{\sin[(g+l+l')A]}{g+l+l'}+K(\omega')\frac{\sin[(g+l-l')A]}{g+l-l'}\right]\right].$$

From this and similar formulas for different combinations of $|\psi^L\rangle$ and $|\psi^R\rangle$ states, one may build up the corresponding matrix elements for fixed parity states. The matrix elements between even and odd quasicontinuum states (in the finite L case) differ mainly by smearing out of singularities by a finite size of the box.

---

*On leave from Institue of Physics, Jagiellonian University, Poland.

[1]L. V. Keldysh, Zh. Eksp. Teor. Fiz. **47**, 1945 (1964) [Sov. Phys.—JETP **20**, 1307 (1965)].

[2](a) A. Gold and H. B. Bebb, Phys. Rev. **143**, 1 (1966); (b) A. M. Perelomov, V. S. Popov, and N. V. Terent'ev, Zh. Eksp. Teor. Fiz. **50**, 1393 (1966) [Sov. Phys.—JETP **23**, 924 (1966)]; **51**, 309 (1967) [**24**, 207 (1967)]; (c) A. M. Perelomov and V. S. Popov, *ibid.* **52**, 514 (1967) [*ibid.* **25**, 336 (1967)].

[3]See, e.g., (a) G. J. Pert, J. Phys. B **8**, L173 (1975); (b) H. S. Brandi, L. Davidovich, and N. Zagury, Phys. Rev. A **24**, 2044 (1981); (c) M. H. Mittleman, *Theory of Laser Atom Interaction* (Plenum, New York, 1983), Chap. 7; (d) H. Reiss, in *Quantum Electrodynamics and Quantum Optics,* edited by A. O. Barut (Plenum, New York, 1984), p. 399.

[4](a) P. Agostini, F. Fabre, G. Mainfray, G. Petite, and N. K. Rahman, Phys. Rev. Lett. **42**, 1127 (1979); (b) P. Kruit, J. Kimman, and M. J. van der Wiel, J. Phys. B **14**, L597 (1981); (c) P. Kruit, J. Kimman, H. G. Muller, and M. J. van der Wiel, Phys. Rev. A **28**, 248 (1983); (d) L. A. Lompre, A. L'Huillier, G. Mainfray, and C. Manus, J. Opt. Soc. Am. B **2**, 1906 (1985).

[5](a) H. G. Muller, A. Tip, and M. J. van der Wiel, J. Phys. B **16**, L679 (1983); (b) H. G. Muller and A. Tip, Phys. Rev. A **20**, 3039 (1984).

[6]For a review on ponderomotive force see (a) J. H. Eberly, Prog. Opt. **7**, 359 (1969); (b) P. Avan, C. Cohen-Tannoudji, J. Dupont-Roc, and C. Fabre, J. Phys. (Paris) **37**, 993 (1976).

[7](a) M. H. Mittleman, Phys. Rev. A **29**, 2245 (1983); (b) A. Szoke, J. Phys. B **18**, L427 (1985); (c) S. I. Chu and J. Cooper, Phys. Rev. A **32**, 2769 (1985); (d) F. Ehlotzky, Can. J. Phys. **63**, 907 (1985); (e) W. Becker, R. R. Schlicher, and M. O. Scully, J. Phys. B **19**, L785 (1986).

[8](a) H. R. Reiss, Phys. Rev. A **22**, 1786 (1980); J. Phys. B **20**, L79, (1987); (b) Z. Bialynicka-Birula, *ibid.* **17**, 3091 (1984).

[9](a) M. Edwards, L. Pan, and L. Armstrong, Jr., J. Phys. B **17**, L515 (1984); *ibid.* **18**, 1927 (1985); (b) Z. Deng and J. H. Eberly, Phys. Rev. Lett. **53**, 1810 (1984); J. Opt. Soc. Am. B **2**, 486 (1985); J. Phys. B **18**, L287 (1985); (c) M. Lewenstein, J. Mostowski, and M. Trippenbach, J. Phys. B **18**, L461 (1985); (d) K. Rzazewski and R. Grobe, Phys. Rev. Lett. **54**, 1729 (1985); Phys. Rev. A **33**, 1855 (1986); (e) J. H. Eberly, Proceedings of the Sixth International School on Coherent Optics, Ustron, 1985 (unpublished).

[10]M. Crance, J. Phys. B **19**, L269 (1986).

[11]F. Yergeau, G. Petite, and P. Agostini, J. Phys. B **19**, L663 (1986).

[12]K. C. Kulander, Phys. Rev. A **35**, 445 (1987).

[13]S. Geltman, J. Phys. B **10**, 831 (1977).

[14]E. J. Austin, J. Phys. B **12**, 4045 (1977).

[15]R. Blumel and R. Meir, J. Phys. B **18**, 2835 (1985).

[16]J. Zakrzewski and K. Zyczkowski, Acta Phys. Pol. A **70**, 807 (1986).

[17]I. L. Mayer, L. C. M. Miranda, B. Y. Tong, and R. M. O. Galvao, J. Phys. B **18**, 3835 (1985).

[18]See, e.g., D. S. Chemla, Phys. Today, **38**(5), 57 (1985) and references therein.

[19](a) A. K. Dhar, M. A. Nagarajan, F. M. Izrailev, and R. R. Whitehead, J. Phys. B **16**, L17 (1983); (b) A. Carnegie, J. Phys. B **17**, 3435 (1984); (c) R. Blumel and U. Smilansky, Phys. Rev. A **30**, 1040 (1984); (d) T. Grozdanov and H. S. Taylor, J. Phys. B (to be published).

[20]M. V. Berry, N. L. Balazs, M. Tabor, and A. Voros, Ann. Phys. (NY) **122**, 26 (1979).

[21](a) G. Casati, B. V. Chirikov, F. M. Izrailev, and J. Ford in Vol. 93 of *Lecture Notes in Physics* (Springer, New York, 1979), p. 333; (b) D. R. Grempel, R. E. Prange, and S. Fishman, Phys. Rev. A **29**, 1639 (1984); (c) S. J. Chang and K. J. Shi, *ibid.* **34**, 7 (1986); (d) G. Casati, J. Ford, I. Guarnieri, and F. Vivaldi, *ibid.* **34**, 1413 (1986); (e) R. Blumel, S. Fishman, and U. Smilansky, J. Chem. Phys. **84**, 2604 (1986).

[22]We were not able to decrease ω_L below $\omega_L = 0.25\,|E_0|$ due to CPU problems; for smaller ω_L (longer filed period) we would have needed to increase the box size L to avoid reflections on box walls.

[23](a) K. Rzazewski, M. Lewenstein, and J. H. Eberly, J. Phys. B **15**, L661 (1982); (b) J. Zakrzewski, K. Rzazewski, and M. Lewenstein, *ibid.* **17**, 729 (1984).

[24]A greater number of peaks appear in the "narrow" well case as the corresponding matrix element decays more slowly with increasing ω.

[25]Coupling of the even-parity bound state to even quasicontinuum functions is much less important being of at least second order in g.

[26]K. Zyczkowski and J. Zakrzewski (unpublished) (available from authors).